SOUND PROPAGATION IN THE PRESENCE OF A LOCALLY-RESONANT SURFACE: AN ANALYTICAL MODEL

L. Schwan Acoustics Research Centre, University of Salford, U.K.
O. Umnova Acoustics Research Centre, University of Salford, U.K.
C. Boutin Ecole Nationale des Travaux Publics de l'Etat, France

1 INTRODUCTION

Surfaces with periodic profiles find many applications in room acoustics and noise control: carefully designed, they can be used as diffusers[1], absorbers[2] or roughness-based scatterers[3]. However, their effects are usually limited to wavelengths of the order of the lattice constant, which requires large structures to affect low frequencies. Besides, array of resonators have been long-known to allow for sound-absorption at low frequencies[4]. Here the concept of a tailored periodic surface with resonant roughness elements is reported. The resonance induces significant changes in the acoustic field in the low frequency range while roughness affects the wavefield at higher frequencies. The present paper focuses on the low-frequency resonant behavior of the corrugated surface; it relies on the existence of a scale separation between the small-size period and the long-wavelength field around the resonance. The system differs from perforated panels[5] since the subwavelength resonators are arranged on or immediately above the surface, thus producing surface corrugation. In particular, it differs from perforated panels with un-partitioned air-backing since, here, the resonators are distinct, each one of them having its own inner dynamics (similarly to panels with partitioned air-backing). The scale separation also distinguishes the resonant surface from sonic crystals[6] or diffraction-based diffusers which require wavelength of the order of the period. Here, due to the subwavelength size of the period, the complex multiple interferences between the resonators are confined within a boundary layer[7,8,9] in the vicinity of the surface. That allows the homogenization[7,10] of the resonant array into an effective surface admittance for the long-wavelength acoustic field. The structure of the paper is as follows. In Section 2, the problem is formulated in the usual framework of the two-scale asymptotic homogenization method. In Section 3, the equivalent surface condition is derived from the leading-order problem. In Section 4, a plane wave reflection from the resonant surface is studied to illustrate its properties.

2 STATEMENT OF THE PROBLEM

The resonant array consists of the 2D Σ-periodic arrangement of identical linear acoustic resonators (volume $\mathcal{V}$) on the surface Γ (inward normal $\mathbf{n}$), as shown in Figure 1, a. The medium above the surface is air. The acoustic properties of the surface Γ are described by the heterogeneous admittance Y which has the same Σ-periodicity as the array.

The propagation of acoustic perturbations is investigated under the ambient conditions – the density of air is $\rho_e = 1.2$ kg/m^3, the atmospheric pressure $P_e = 1.013 \times 10^5$ Pa, the adiabatic constant $\gamma = 1.4$ and the sound speed $c = \sqrt{\gamma P_e / \rho_e} \approx 343.3$ m/s. Viscous and thermal losses are neglected in the air but the damping is accounted for within the resonators.

The analysis is performed in the harmonic regime at frequencies $f = \omega/2\pi$ close enough to the eigenfrequency $\omega_o/2\pi$ of the resonators i.e. $\omega \approx \omega_o$. Time dependence in the form $e^{-i\omega t}$ is used throughout the paper. In the frequency range considered, a scale separation is assumed whereby the size ℓ of the period Σ is much smaller than the wavelength of sound $\lambda = c/f = 2\pi/k$. That introduces the small scale-parameter $\varepsilon = k\ell \ll 1$ used in further derivations.

Due to scale separation a regime of "co-dynamics" is achieved[11] between the subwavelength resonant structures on the surface and the long-wavelength fields in the halfspace. Indeed, in response to pressure disturbance that prevails in the halfspace, velocity $\boldsymbol{V}$ is imposed on the boundary $\partial\mathcal{V}$ of each resonator. This velocity is governed by the resonator's own inner dynamics. Thus, the resonators contribute to the mass balance in the system as secondary acoustic sources. Since $\boldsymbol{V}$ is forced by the long-wavelength field, it varies at the long-wavelength scale. But, because of the scale separation and of the Σ-periodicity of the array, $\boldsymbol{V}$ varies also at the subwavelength scale and satisfies the local Σ-periodicity.

As a result of the double-scale variations of $\boldsymbol{V}$, the total acoustic field in the half-space also varies at both the long-wavelength and the subwavelength scales. However, due to the scale separation, subwavelength variations of the fields are expected to remain located near their sources (i.e. the resonators) and vanish away from them. This leads to the development of a Σ-periodic boundary layer close to the resonators, while away from them, only long-wavelength variations remain in the fields. Moreover, as the resonant array is positioned nearby the boundary Γ of the halfspace i.e. at a distance h from Γ so that $h = O(\ell) = O(\varepsilon k^{-1})$, the boundary layer remains confined to the vicinity of the surface Γ.

3 TWO-SCALE ASYMPTOTIC FORMULATION

Taking advantage of the existence of the small scale-parameter $\varepsilon \ll 1$, the problem is formulated in the usual framework of two-scale asymptotic homogenization[7,9,10]. Firstly, two space variables $\boldsymbol{x}$ and $\boldsymbol{y} = \varepsilon^{-1}\boldsymbol{x}$ are introduced, associated respectively with the long-wavelength and subwavelength variations in the fields. The use of two distinct space variables modifies the spatial differential operator into $\partial = \partial_{\boldsymbol{x}} + \varepsilon^{-1}\partial_{\boldsymbol{y}}$ where $\partial_{\boldsymbol{x}}$ and $\partial_{\boldsymbol{y}}$ are derivatives with respect to $\boldsymbol{x}$ and $\boldsymbol{y}$ respectively. Secondly, the fields are expanded asymptotically in powers of $\varepsilon \ll 1$ e.g. the velocity field $\boldsymbol{V}$ is expanded as $\boldsymbol{V} = \boldsymbol{V}^{(0)} + \varepsilon^1\boldsymbol{V}^{(1)} + \varepsilon^2\boldsymbol{V}^{(2)} + \cdots$, where the exponent in brackets indicates the order of the terms. These expansions are then introduced in mass and momentum conservation equations and in boundary conditions, expressed using the generalized differential operators ∂. The terms with equal powers of ε are collected, providing problems that are solved in increasing order of ε-powers. The leading term ε^0 and the correctors to the fields are thus obtained.

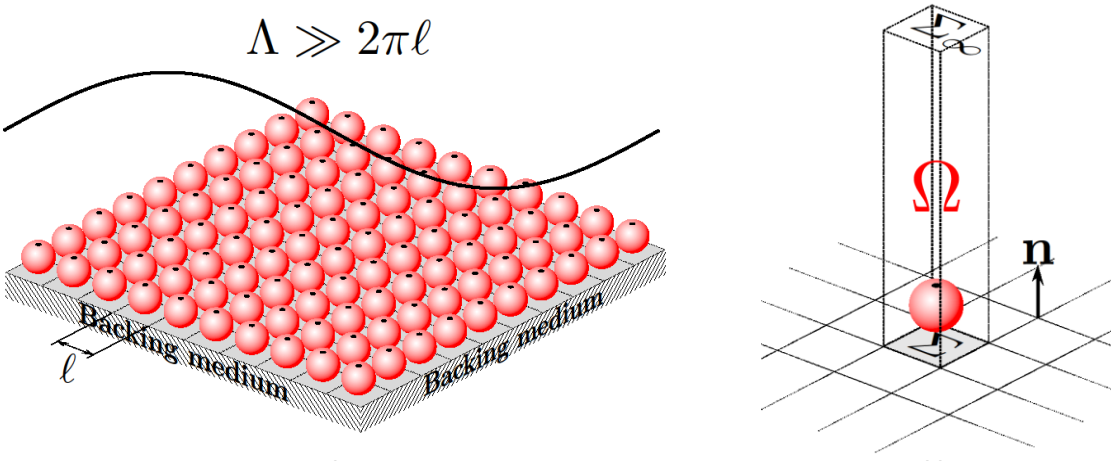

a) b)

Figure 1: Periodic array of resonators above a plane surface: a) schematic view of the system under scale separation whereby the array period is much smaller than the wavelength of sound; b) column Ω of air above one period.

The total acoustic field in the half-space, with the particle velocity $\boldsymbol{v}_t(\boldsymbol{x},\boldsymbol{y})$ and the pressure disturbance $p_t(\boldsymbol{x},\boldsymbol{y})$ that depend on both space variables $\boldsymbol{x}$ and $\boldsymbol{y}$, satisfies equations of mass and momentum conservation (expressed with the generalized derivatives) and the boundary conditions i.e. the velocity $\boldsymbol{V}(\boldsymbol{x},\boldsymbol{y}) = \boldsymbol{V}^{(0)}(\boldsymbol{x},\boldsymbol{y}) + \varepsilon^1\boldsymbol{V}^{(1)}(\boldsymbol{x},\boldsymbol{y}) + \varepsilon^2\boldsymbol{V}^{(2)}(\boldsymbol{x},\boldsymbol{y}) + \cdots$ is balanced on the boundary $\partial\mathcal{V}$ of each resonator and the admittance $Y(\boldsymbol{y})$ on $\Sigma \subset \Gamma$ is matched:

$$\left(\mathrm{div}_{\boldsymbol{x}} + \varepsilon^{-1}\,\mathrm{div}_{\boldsymbol{y}}\right)\boldsymbol{v}_t(\boldsymbol{x},\boldsymbol{y}) = \frac{i\,\omega}{\gamma\,P_e}\,p_t(\boldsymbol{x},\boldsymbol{y})\,, \tag{1a}$$

$$i\omega\rho_e\,\boldsymbol{v}_t(\boldsymbol{x},\boldsymbol{y}) = \left(\mathbf{grad}_{\boldsymbol{x}} + \varepsilon^{-1}\,\mathbf{grad}_{\boldsymbol{y}}\right)p_t(\boldsymbol{x},\boldsymbol{y}), \tag{1b}$$

$$\boldsymbol{v}_t(\boldsymbol{x},\boldsymbol{y}).\mathbf{n}_{\boldsymbol{y}} = \boldsymbol{V}(\boldsymbol{x},\boldsymbol{y}).\mathbf{n}_{\boldsymbol{y}} \quad \text{on } \partial\mathcal{V}\,, \tag{1c}$$

$$\boldsymbol{v}_t(\boldsymbol{x},\boldsymbol{y}).\mathbf{n} = Y(\boldsymbol{y})\,p_t(\boldsymbol{x},\boldsymbol{y}) \quad \text{on } \Sigma \subset \Gamma. \tag{1d}$$

This total acoustic field is decomposed into: the long-wavelength fields $\boldsymbol{v}(\boldsymbol{x})$ and $p(\boldsymbol{x})$ and the boundary layer fields $\boldsymbol{v}_{\#}(\boldsymbol{x},\boldsymbol{y})$ and $p_{\#}(\boldsymbol{x},\boldsymbol{y})$. Both the long-wavelength fields and the boundary layer fields are defined everywhere (and in particular in the vicinity of the resonant array on Γ) but, far from Γ only the long-wavelength fields prevail:

$$\boldsymbol{v}_t(\boldsymbol{x},\boldsymbol{y}) = \boldsymbol{v}(\boldsymbol{x}) + \boldsymbol{v}_{\#}(\boldsymbol{x},\boldsymbol{y}) \quad \text{with} \quad \boldsymbol{v}_{\#}(\boldsymbol{x},\boldsymbol{y}.\mathbf{n}\to\infty) = \mathbf{0}\,, \tag{2a}$$

$$p_t(\boldsymbol{x},\boldsymbol{y}) = p(\boldsymbol{x}) + p_{\#}(\boldsymbol{x},\boldsymbol{y}) \quad \text{with} \quad p_{\#}(\boldsymbol{x},\boldsymbol{y}.\mathbf{n}\to\infty) = 0\,. \tag{2b}$$

Taking the limit $\boldsymbol{y}.\mathbf{n}\to\infty$ in equation (1) the long-wavelength fields $\boldsymbol{v}(\boldsymbol{x})$ and $p(\boldsymbol{x})$ satisfy the usual equations of mass and momentum conservation with the derivatives $\partial_{\boldsymbol{x}}$ only:

$$\mathrm{div}_{\boldsymbol{x}}\,\boldsymbol{v}(\boldsymbol{x}) = \frac{i\,\omega}{\gamma\,P_e}\,p(\boldsymbol{x}), \tag{3a}$$

$$i\omega\rho_e\,\boldsymbol{v}(\boldsymbol{x}) = \mathbf{grad}_{\boldsymbol{x}}\,p(\boldsymbol{x}). \tag{3b}$$

However, the boundary conditions applied to $\boldsymbol{v}(\boldsymbol{x})$ and $p(\boldsymbol{x})$ are still missing from the analysis since these fields cannot produce the subwavelength periodic variations of the properties near the surface Γ. This transition of scales is realized by the boundary layer fields, where the particle velocity $\boldsymbol{v}_{\#}(\boldsymbol{x},\boldsymbol{y})$ and pressure disturbance $p_{\#}(\boldsymbol{x},\boldsymbol{y})$ depend on both space variables. Subtracting equation (3) from (1), the equations governing the boundary layer near Γ are derived:

$$\left(\mathrm{div}_{\boldsymbol{x}} + \varepsilon^{-1}\,\mathrm{div}_{\boldsymbol{y}}\right)\boldsymbol{v}_{\#}(\boldsymbol{x},\boldsymbol{y}) = \frac{i\,\omega}{\gamma\,P_e}\,p_{\#}(\boldsymbol{x},\boldsymbol{y})\,, \tag{4a}$$

$$i\omega\rho_e\boldsymbol{v}_{\#}(\boldsymbol{x},\boldsymbol{y}) = \left(\mathbf{grad}_{\boldsymbol{x}} + \varepsilon^{-1}\,\mathbf{grad}_{\boldsymbol{y}}\right)p_{\#}(\boldsymbol{x},\boldsymbol{y}), \tag{4b}$$

$$\left(\boldsymbol{v}(\boldsymbol{x}) + \boldsymbol{v}_{\#}(\boldsymbol{x},\boldsymbol{y})\right)\mathbf{n}_{\boldsymbol{y}} = \boldsymbol{V}(\boldsymbol{x},\boldsymbol{y}).\mathbf{n}_{\boldsymbol{y}} \quad \text{on } \partial\mathcal{V}, \tag{4c}$$

$$\left(\boldsymbol{v}(\boldsymbol{x}) + \boldsymbol{v}_{\#}(\boldsymbol{x},\boldsymbol{y})\right)\mathbf{n} = Y(\boldsymbol{y})\,(\,p(\boldsymbol{x}) + p_{\#}(\boldsymbol{x},\boldsymbol{y})\,) \quad \text{on } \Sigma \subset \Gamma. \tag{4d}$$

For the boundary layer to play a significant role in the mass balance, the condition $\boldsymbol{v}_{\#} = O(\boldsymbol{v})$ has to be satisfied. As a result, the boundary layer pressure field $p_{\#}(y)$ is necessarily of the order $p_{\#} = O(\varepsilon p)$, see equation (4b). That means that the pressure field that prevails in the halfspace (up to the order ε) exhibits only the long-wavelength variations despite the presence of subwavelength heterogeneities nearby Γ.

Finally, taking into consideration the orders of magnitude, the fields are expanded asymptotically as:

$$\boldsymbol{v}(\boldsymbol{x}) = \boldsymbol{v}^{(0)}(\boldsymbol{x}) + \varepsilon^1\boldsymbol{v}^{(1)}(\boldsymbol{x}) + \varepsilon^2\boldsymbol{v}^{(2)}(\boldsymbol{x}) + \cdots, \tag{5a}$$

$$p(\boldsymbol{x}) = p^{(0)}(\boldsymbol{x}) + \varepsilon^1 p^{(1)}(\boldsymbol{x}) + \varepsilon^2 p^{(2)}(\boldsymbol{x}) + \cdots\,, \tag{5b}$$

$$\boldsymbol{v}_{\#}(\boldsymbol{x},\boldsymbol{y}) = \boldsymbol{v}_{\#}^{(0)}(\boldsymbol{x},\boldsymbol{y}) + \varepsilon^1\boldsymbol{v}_{\#}^{(1)}(\boldsymbol{x},\boldsymbol{y}) + \varepsilon^2\boldsymbol{v}_{\#}^{(2)}(\boldsymbol{x},\boldsymbol{y}) + \cdots\,, \tag{5c}$$

$$p_{\#}(\boldsymbol{x},\boldsymbol{y}) = \varepsilon^1 p_{\#}^{(1)}(\boldsymbol{x},\boldsymbol{y}) + \varepsilon^2 p_{\#}^{(2)}(\boldsymbol{x},\boldsymbol{y}) + \cdots\,, \tag{5d}$$

$$\boldsymbol{V}(\boldsymbol{x},\boldsymbol{y}) = \boldsymbol{V}^{(0)}(\boldsymbol{x},\boldsymbol{y}) + \varepsilon^1\boldsymbol{V}^{(1)}(\boldsymbol{x},\boldsymbol{y}) + \varepsilon^2\boldsymbol{V}^{(2)}(\boldsymbol{x},\boldsymbol{y}) + \cdots\,. \tag{5e}$$

4 EQUIVALENT SURFACE CONDITION AT LEADING ORDER

The effective surface condition for the long-wavelength field $\{\boldsymbol{v}^{(0)};\, p^{(0)}\}$ is derived from equations (4) where the asymptotic expansions (5) have been introduced. At the leading order ε^0, they read:

$$\mathrm{div}_{\boldsymbol{y}}\, \boldsymbol{v}_{\#}^{(0)}(\boldsymbol{x},\boldsymbol{y}) = 0, \tag{6a}$$

$$\left(\boldsymbol{v}^{(0)}(\boldsymbol{x}) + \boldsymbol{v}_{\#}^{(0)}(\boldsymbol{x},\boldsymbol{y})\right)\mathbf{n}_{\boldsymbol{y}} = \boldsymbol{V}(\boldsymbol{x},\boldsymbol{y}).\mathbf{n}_{\boldsymbol{y}} \qquad \text{on } \partial\mathcal{V}, \tag{6b}$$

$$\left(\boldsymbol{v}^{(0)}(\boldsymbol{x}) + \boldsymbol{v}_{\#}^{(0)}(\boldsymbol{x},\boldsymbol{y})\right)\mathbf{n} = Y(\boldsymbol{y})\, p^{(0)}(\boldsymbol{x}) \qquad \text{on } \Sigma. \tag{6c}$$

Equation (6a) shows that the flow within the boundary layer is quasi-incompressible at the leading order ε^0. This implies that the thickness of the boundary layer is of order ε compared to the long-wavelength. Integrate equation (6a) over the column Ω of air above one period Σ, as shown in Figure 1, b, and apply the divergence theorem. The boundary $\partial\Omega$ of Ω consists of the period $\Sigma \subset \Gamma$, the lateral face Σ_{lat}, the section Σ_∞ located at $\boldsymbol{y}.\mathbf{n} \to \infty$ and the boundary $\partial\mathcal{V}$ of the resonator. Thus:

$$\int_\Omega \mathrm{div}_{\boldsymbol{y}}\, \boldsymbol{v}_{\#}^{(0)}(\boldsymbol{x},\boldsymbol{y})\ \mathrm{d}\Omega_{\boldsymbol{y}} = \int_{\partial\mathcal{V}\cap\Sigma\cap\Sigma_\infty\cap\Sigma_{\mathrm{lat}}} \boldsymbol{v}_{\#}^{(0)}(\boldsymbol{x},\boldsymbol{y})\,.\,\mathbf{n}_{\boldsymbol{y}}\,\mathrm{d}S_{\boldsymbol{y}} = 0\,. \tag{7}$$

Due to the Σ-periodicity and evanescence ($\boldsymbol{v}_{\#}(\boldsymbol{x},\Sigma_\infty) \to \mathbf{0}$) of $\boldsymbol{v}_{\#}^{(0)}(\boldsymbol{x},\boldsymbol{y})$, both the contributions on Σ_{lat} and Σ_∞ cancel out. As for the long-wavelength field $\boldsymbol{v}^{(0)}(\boldsymbol{x})$, which is quasi-uniform on $\Omega(\boldsymbol{y})$, its flux cancels out on $\partial\mathcal{V}$ since it is a regular closed surface ($\int_{\partial\mathcal{V}} \mathbf{n}_{\boldsymbol{y}}\ \mathrm{d}S_{\boldsymbol{y}} = \mathbf{0}$) and its flux on $\Sigma \subset \Gamma$ is $|\Sigma|\boldsymbol{v}^{(0)}(\boldsymbol{x}).\mathbf{n}$. Consequently the following equations hold

$$\int_{\partial\mathcal{V}\cap\Sigma} \boldsymbol{v}_{\#}^{(0)}(\boldsymbol{x},\boldsymbol{y}).\mathbf{n}_{\boldsymbol{y}}\ \mathrm{d}S_{\boldsymbol{y}} = 0 \qquad ; \qquad \int_{\partial\mathcal{V}\cap\Sigma} \boldsymbol{v}^{(0)}(\boldsymbol{x}).\mathbf{n}_{\boldsymbol{y}}\ \mathrm{d}S_{\boldsymbol{y}} = |\Sigma|\boldsymbol{v}^{(0)}(\boldsymbol{x}).\mathbf{n}\,. \tag{8}$$

On the other hand, the flux from $\partial\mathcal{V} \cap \Sigma$ is given by the boundary conditions in equations (6b-c):

$$\int_{\partial\mathcal{V}\cap\Sigma} \left(\boldsymbol{v}^{(0)}(\boldsymbol{x}) + \boldsymbol{v}_{\#}^{(0)}(\boldsymbol{x},\boldsymbol{y})\right)\mathbf{n}_{\boldsymbol{y}}\ \mathrm{d}S_{\boldsymbol{y}} = \int_{\partial\mathcal{V}} \boldsymbol{V}^{(0)}(\boldsymbol{x},\boldsymbol{y}).\mathbf{n}_{\boldsymbol{y}}\,\mathrm{d}S_{\boldsymbol{y}} + \int_\Sigma Y(\boldsymbol{y})\,\mathrm{d}S_{\boldsymbol{y}}\ p^{(0)}(\boldsymbol{x})\,. \tag{9}$$

Define the flux $q^{(0)}(\boldsymbol{x}) = \int_{\partial\mathcal{V}} \boldsymbol{V}^{(0)}(\boldsymbol{x},\boldsymbol{y}).\mathbf{n}_{\boldsymbol{y}}\,\mathrm{d}S_{\boldsymbol{y}}$ emitted by the resonator into the half-space and the mean admittance $\langle Y\rangle = \frac{1}{|\Sigma|}\int_\Sigma Y(\boldsymbol{y})\,\mathrm{d}S_{\boldsymbol{y}}$ on the array period. Combining equations (8-9), the equivalent boundary condition for the long-wavelength field yields

$$\boldsymbol{v}^{(0)}(\boldsymbol{x}).\mathbf{n} = \frac{q^{(0)}(\boldsymbol{x})}{|\Sigma|} + \langle Y\rangle\, p^{(0)}(\boldsymbol{x})\ . \tag{10}$$

At the leading order, the long-wavelength field balances the total flux produced in the vicinity of Γ per unit area of the two dimensional period Σ. Since only the flux is significant, the condition does require neither the exact knowledge of the geometry of the resonator nor that of the velocity $\boldsymbol{V}^{(0)}$ or the admittance $Y(\boldsymbol{y})$. In particular, roughness affects only the terms of order ε^1 and total fluxes of value zero (e.g. a distribution of acoustic moments) have no direct influence, at the leading order, on the macroscopic field. Moreover, perturbations of the periodic arrangement produce no significant effects at the leading order, conversely to sonic crystal arrays[12]. Finally, note that equation (9) follows directly from the balance within the boundary layer and relies upon its properties of quasi-incompressible flow, periodicity and evanescence at the leading order. Since no use has been made of the momentum conservation within the boundary layer, the result remains valid even if the viscosity of the gas in the half-space is accounted for. As the analysis below is limited to the leading order, the exponent (0) indicating the order of the fields is omitted.

The resonator $(\mathcal{V})$ emits the flux $q(\boldsymbol{x})$ in response to the pressure field that acts on it. At the leading order, this latter is dominated by the long-wavelength field $p(\boldsymbol{x})$. Since the resonator is linear, $q(\boldsymbol{x})$ is therefore related to $p(\boldsymbol{x})$ by a frequency-dependent admittance Y_o so that $q(\boldsymbol{x}) = |\Sigma|Y_o p(\boldsymbol{x})$.

To illustrate the properties of Y_o, suppose that the resonator has a rigid boundary except for an aperture A where a piston-like motion of gas produces the flux $q(\boldsymbol{x})$ and can be described as a single degree of freedom oscillator. It is characterized by mass M, stiffness K and the damping coefficient C. The harmonic pressure $p(\boldsymbol{x})$ induces the velocity $V_o = q/|A|$ of the mass M according to the second Newton's law:

$$-i\omega\, M\, V_o = |A|\,(p_o - p) \qquad \text{with} \qquad |A|\, p_o = -(K - i\omega\, C)\, \frac{V_o}{-i\omega}\ . \tag{11}$$

where p_o represents the characteristic pressure inside the resonator. Defining the eigenfrequency $\omega_o = \sqrt{K/M}$ and assuming weak damping $\xi_o = C/2\sqrt{KM} \ll 1$, the admittance $Y_o = |A|V_o/|\Sigma|p$ at the aperture of the resonator and the transfer function p_o/p read:

$$Y_o = \frac{|A|}{|\Sigma|}\frac{i\omega|A|/K}{1 - i2\xi_o\omega/\omega_o - \omega^2/\omega_o^2} \qquad \text{and} \qquad p_o = \frac{1}{1 - i2\xi_o\omega/\omega_o - \omega^2/\omega_o^2}\, p\ . \tag{12}$$

Combining this result with equation (10) shows that the resonant surface can be described by the equivalent admittance $Y_\Gamma = Y_o + \langle Y\rangle$, so that $\boldsymbol{v}^{(0)}(\boldsymbol{x}).\mathbf{n} = Y_\Gamma\, p^{(0)}(\boldsymbol{x})$. Normalized by the admittance $Y_e = 1/\rho_e c$ of air it takes the following form

$$\frac{Y_\Gamma}{Y_e} = \eta\, \frac{i\omega/\omega_o}{1 - i2\xi_o\omega/\omega_o - \omega^2/\omega_o^2} + \frac{\langle Y\rangle}{Y_e} \qquad \text{with} \qquad \eta = \frac{|A|}{|\Sigma|}\frac{\sqrt{\gamma P_e \rho_e}}{\sqrt{K\,M}\,/|A|}\,. \tag{13}$$

The following asymptotics are derived for the admittance in the low and high frequency ranges and around the resonance

$$\frac{Y_\Gamma}{Y_e} \xrightarrow[\omega \ll \omega_o]{} \frac{i\omega}{\omega_o}\eta + \frac{\langle Y\rangle}{Y_e} \quad ; \quad \frac{Y_\Gamma}{Y_e} \xrightarrow[\omega \gg \omega_o]{} \frac{\omega_o}{i\omega}\eta + \frac{\langle Y\rangle}{Y_e} \quad ; \quad \frac{Y_\Gamma}{Y_e} \xrightarrow[\omega \approx \omega_o]{} -\frac{\eta}{2\xi_o} + \frac{\langle Y\rangle}{Y_e}\,. \tag{14}$$

Far from the resonance ($\omega \ll \omega_o$ or $\omega \gg \omega_o$) the admittance contribution Y_o from the resonator is negligible and the boundary condition is dominated by the surface admittance $\langle Y\rangle$. On the contrary, around the resonance $\omega \approx \omega_o$ of undamped resonators ($\xi_o = 0$) the admittance Y_o of the resonator becomes infinite $Y_o \to -\infty$ having the same effect as the “pressure release” surface condition. Of course, the damping of the resonator changes this behavior removing the singularity, but still the transition from one surface admittance to another occurs in the frequency range around resonance.

5 WAVE REFLECTION FROM THE RESONANT SURFACE

To illustrate the effects of the resonant surface, the reflection of a plane wave with the amplitude p_i incident on the resonant surface at an angle $-\theta$ with the normal $\mathbf{n}$ is analysed. According to Descartes' law, a plane wave with amplitude p_r is reflected from the surface in the direction making the angle $+\theta$ with $\mathbf{n}$. The superposition of the incident and reflected waves must satisfy boundary conditions on the surface described by the effective admittance Y_Γ derived in the previous section. This leads to the following expression for the reflection coefficient $R = p_r/p_i$:

$$Y_e(p_i - p_r)\cos\theta = Y_\Gamma\,(p_i + p_r) \qquad \Longrightarrow \qquad R = \frac{p_r}{p_i} = \frac{\cos\theta + Y_\Gamma/Y_e}{\cos\theta - Y_\Gamma/Y_e}\ . \tag{15}$$

To emphasize the effect of the resonators and to simplify the calculations, it is assumed that $\langle Y\rangle = 0$ in equation (13) i.e. the resonant array is arranged above or on the rigid surface. The frequency dependences of the amplitude and the phase of the reflection coefficient R are presented in Figures 2, a, b, where the influence of the angle of incidence and damping is also shown. While the low and high frequency limits are analogous to those of a rigid surface ($R \approx 1$), a phase shift occurs around resonance. The amplitude of R is sensitive to the resonators' damping ξ_o : for undamped resonators ($\xi_o = 0$), the admittance Y_Γ is purely imaginary leading to a total reflection of the wave ($|R| = 1$) at any frequency, while for damped resonators ($\xi_o \neq 0$), Y_Γ has a non-zero real part that leads to a

partial reflection ($|R| \leq 1$) of the incident wave. Note that the existence of even weak damping ξ_o, leads to vanishing the reflected wave ($R \to 0$) around the resonance ($Y_\Gamma/Y_e = -\eta/2\xi_o$) for $\cos\theta = \eta/2\xi_o \leq 1$. In this case the resonant surface acts then as a fully absorbing layer. The effect of the resonant surface on pressure p_Γ immediately on the surface Γ is even more pronounced:

$$p_\Gamma = (1+R)\, p_i = \frac{2\cos\theta}{\cos\theta - Y_\Gamma/Y_e} p_i = 2\, \frac{1 - i2\xi_o\omega/\omega_o - \omega^2/\omega_o^2}{1 - i2\,\zeta\omega/\omega_o - \omega^2/\omega_o^2}\, p_i \quad \text{where} \quad \zeta = \xi_o + \frac{\eta}{2\cos\theta}\ . \tag{16}$$

While out of resonance p_Γ is twice the incident pressure (similarly to a rigid-surface condition and consistently with $Y_\Gamma/Y_e \ll 1$), its amplitude is strongly reduced around the resonant frequency, whether the resonators are undamped ($\xi_o = 0,\ Y_\Gamma/Y_e \to -\infty$ and the surface is pressure-free) or weakly-damped (producing a finite contrast of admittances $Y_\Gamma/Y_e = -\eta/2\xi_o$). These features are shown in Figures 2, c, d. Note that when the angle of incidence θ increases, the pressure p_Γ on the surface decreases significantly around resonance. The convolution of pressure p_Γ in equation (16) with the transfer function of the resonator in equation (11) yields

$$p_o(t) = \frac{2}{1 - i2\,\zeta\omega/\omega_o - \omega^2/\omega_o^2}\, p_i(t)\ . \tag{19}$$

As shown in Figures 2, e, f, at resonance the pressure inside the resonator remains finite even for undamped resonators - for $\xi_o = 0,\ \ p_o/p_i = i\,2cos\theta/\eta$ at resonance $\omega = \omega_o$. Since the system is non-dissipative, the apparent damping $\eta/2cos\theta$ is due to the radiation from the resonators.

Finally, in the time domain, for a unitary Dirac-function incident signal, pressure on the surface is given by the inverse Fourier transform of equation (16). For $\zeta < 1$ it yields

$$p_\Gamma(t) = 2\left(1 + \frac{2\xi_o}{\omega_o}\frac{\partial}{\partial t} + \frac{1}{\omega_o^2}\frac{\partial^2}{\partial t^2}\right)\frac{\omega_o}{\sqrt{1-\zeta^2}}\sin(\omega_o\sqrt{1-\zeta^2}\,t)\ e^{-\zeta\omega_o t}. \tag{17}$$

Instead of a Dirac-function response, as would be the case for a rigid surface, the resonant surface response is transient i.e. $p_\Gamma(t)$: it oscillates with the frequency $\omega_o\sqrt{1-\zeta^2}$ and decreases exponentially with the characteristic time $1/\zeta\omega_o$. This phenomenon is illustrated in Figure 3 for a more realistic incident Ricker impulse (central frequency $\omega_R = \omega_o$ and time-delay $t_0 = 4\pi/\omega_o$) defined as

$$p_i(t) = (2A^2(t) - 1)e^{-A^2(t)} \qquad \text{where} \qquad A(t) = \frac{\omega_r(t-t_0)}{2}. \tag{18}$$

This "memory effect" is noticeable away from the resonators where the reflected field still keeps information about the boundary condition.

6 CONCLUSION

The concept of microstructured surface with resonant roughness elements is reported. The properties of a resonator array arranged in the vicinity of an admittance surface has been described, under scale separation, by an equivalent admittance. The reflection of waves from the surface leads, around resonance, to a phase-shift in the reflected wavefield, possibly with vanishing amplitude, a decrease of pressure on the surface, a radiation damping for the resonators and a surface memory effect in the time domain. The derivation relies strongly on the existence of the boundary layer near the array and the application of the two-scale asymptotic homogenization method to derive the equivalent boundary condition (usually, the two-scale homogenization procedure is used to describe the behaviour of 3D heterogeneous media). This formulation offers the possibility of improving the leading order description by considering higher order terms in the asymptotic expansion (in particular when the scale separation is not sharp) and the frequency range of its application is derived without any ambiguities.

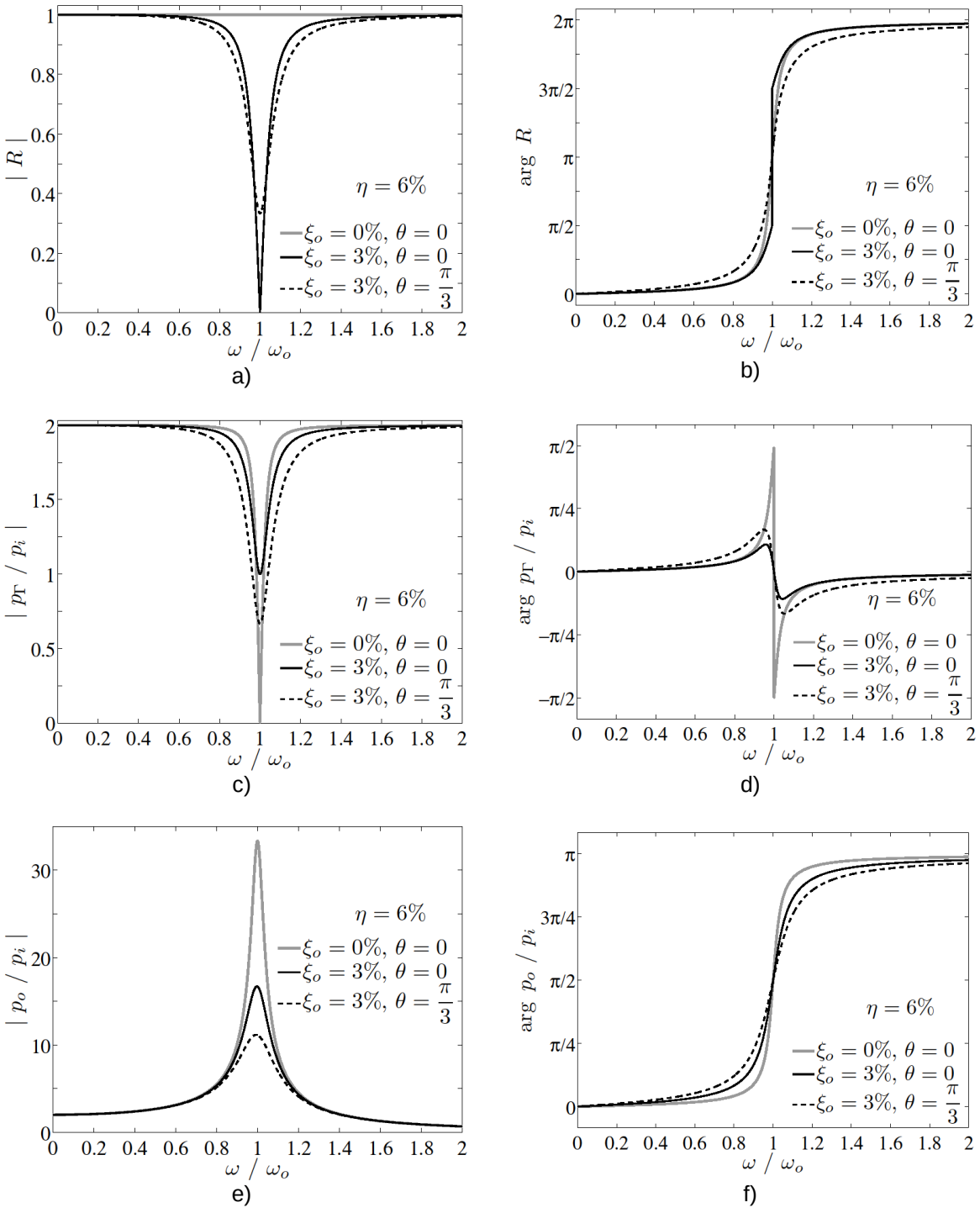

Figure 2: Plane wave reflection from the resonant surface in the frequency domain. Modulus and phase against the frequency (normalized by the eigenfrequency of the resonators) of: a-b) the reflection coefficient; c-d) the pressure p_Γ on the surface normailized by the incident amplitude; e-f) the characteristic pressure p_o inside the resonator. Calculations with $\eta = 6\%$, for damped ($\xi_o = 3\%$) or undamped ($\xi_o = 0$) resonators and for normal ($\theta = 0$) of oblique ($\theta = \pi/3$) incidence.

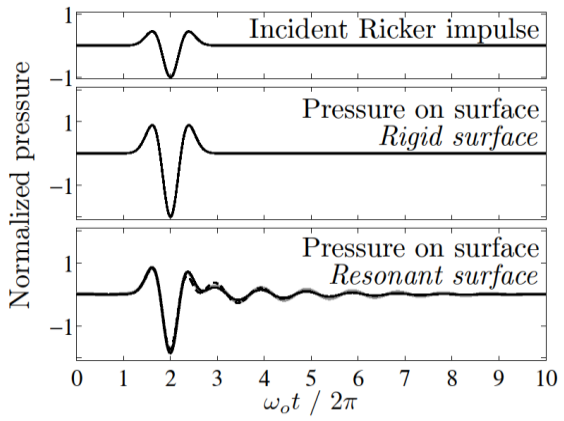

Figure 3: Time-response of the resonant surface to an incident Ricker impulse. Top: signal of the incident Ricker impulse (normalized to 1); middle: signal of the pressure p_Γ on a rigid surface (twice the incident signal); bottom: signal of the pressure p_Γ on the resonant surface for different damping and angle of incidence. These latter are obtained by convolution of the incident Ricker impulse with the transfer functions in figures 2c)-2d). Same legend as figures 2c)-2d).

The model does not require any assumptions about the geometry of the resonators or the source, as long as the scale separation is satisfied. It allows considering more complex arrangements than the one presented in this paper, such as combining several oscillators of different nature in a period (e.g. resonators with different eigenfrequencies, or arranging an array of Helmholtz resonators nearby a perforated panel, etc) ; using resonators with exotic shapes; using more complex sources (homogeneous or inhomogeneous waves, plane, cylindrical or spherical waves etc). Moreover, under scale separation, periodic and non-periodic arrangements provide similar results[10]. The analytical formulation allows parametric studies at very low computational cost and straightforward designs. Designs have already been suggested to build resonators that satisfy the scale separation at their resonance[11]. An experimental campaign is planned to validate the predicted results.

7 REFERENCES

1. M. R. Schroeder, 'Binaural dissimilarity and optimum ceilings for concert halls: More lateral sound diffusion', J. Acoust. Soc. Am. 65(4) 958-963 (1979)
2. F.P. Mechel, 'The wide-angle diffuser – a wide-angle absorber?', Acustica (81) 379-401 (1995)
3. I. Bashir, S. Taherzadeh and K. Attenborough, 'Diffraction assisted rough ground effect: Models and data', J. Acoust. Soc. Am. 133(3) 1281-1292 (2013)
4. V.-L. Jordan, 'The application of Helmholtz resonators to sound-absorbing structures', J. Acoust. Soc. Am. 19(6) 972-981 (1947)
5. D.-Y. Maa, 'Potential of microperforated panel absorber', J. Acoust. Soc. Am. 104(5) 2861-2866 (1998)
6. A. Krynkin, et al., 'Acoustic insertion loss due to two dimensional periodic arrays of circular cylinders parallel to a nearby surface', J. Acoust. Soc. Am. 130(6) 3736-3745 (2011)
7. E. Sanchez-Palencia, 'Nonhomogeneous media and vibration theory', Lecture Notes in Physics, vol. 127, Springer-Verlag Berlin, 400 pages (1980)
8. C.L. Holloway and E.F. Kuester, 'Equivalent boundary conditions for a perfectly conducting periodic surface with a cover layer', Radio Science 35(3) 661-681 (2000)
9. C. Boutin and P. Roussillon, 'Wave propagation in presence of oscillators on the free surface', Int. J. of Eng. Sci. 44 180-204 (2006)
10. J.-L. Auriault, C. Boutin and C. Geindreau, 'Homogenization of coupled phenomena in heterogenous media', ISTE and Wiley, 476 pages (2009)
11. C. Boutin, 'Acoustics of porous media with inner resonance, J. Acoust. Soc. Am. 134(6) 4717-4729 (2013)
12. S. Taherzadeh, I. Bashir and K. Attenborough, 'Aperiodicity effects on sound transmission through arrays of identical cylinders perpendicular to the ground', J. Acoust. Soc. Am. 132(4) EL323-328 (2012)